Journal of Statistical Physics, Vol. 39, Nos. 5/6, 1985

Solitons in Josephson Junctions: An Overview

P. S. Lomdahl[1]

The dynamics of the Josephson tunnel junction is approximately described by a perturbed sine-Gordon equation. The Josephson tunnel junction is thus a convenient experimental solid state device for the study of solitons and solitonlike phenomena. The physical manifestation of the soliton is a propagating magnetic flux quantum ($\Phi_0 = h/2e = 2.064 \times 10^{-15}$ V sec). Basic properties of the soliton and its relation to observable experimental quantities (zero field steps, microwave radiation, etc.) are reviewed. Recent direct measurements of the actual soliton profile are also mentioned.

KEY WORDS: Solitons; nonlinear waves; Josephson junctions; quasi one-dimensional systems.

1. INTRODUCTION

Josephson junctions devices have over the last ten years proven to be one of the most successful testing grounds for nonlinear wave theory. More specifically, a model based on the perturbed sine-Gordon equation has been shown to describe the internal dynamics of the junction very accurately. In this introductory overview I will review the model and show how solitons manifest themselves and how they relate to experimentally observable quantities. Focus will be on the basic properties and, rather than trying to review the very extensive literature on the subject, I will give reference to key papers which can lead the interested reader into more specialized aspects.

The outline of the paper is as follows: In Section 2 the model is derived and in Section 3 contact is made with experiments. Here recent direct

[1] Center for Nonlinear Studies, Los Alamos National Laboratory, Los Alamos, New Mexico 87545.

0022-4715/85/0600-0551$04.50/0

measurements of the soliton profile are also mentioned. Finally in Section 4 a brief conclusion and an outlook is given.

2. MODEL EQUATIONS

Josephson tunnel junctions come in different geometries—here I will focus on the so-called overlap type. Various other geometries are possible (see, e.g., Ref. 1, which is also a good introductory textbook to the field); the model equations will, however, turn out to be very similar to those derived below.

An overlap geometry Josephson tunnel junction consists of two superconducting metal layers separated by a thin insulating oxide layer of uniform thickness which is small enough to permit quantum mechanical tunneling of electrons. The geometry is shown in Fig. 1. The tunneling supercurrent is described by the two basic Josephson equations

$$j = j_J \sin \varphi \tag{1a}$$

$$\frac{\partial \varphi}{\partial t} = \frac{2e}{\hbar} V \tag{1b}$$

where $\varphi = \varphi(x, y, t)$ is the difference between the phases of the order parameters of the two superconductors, $j = j(x, y, t)$ is the Josephson current crossing the insulating layer per unit area, j_J being the maximum

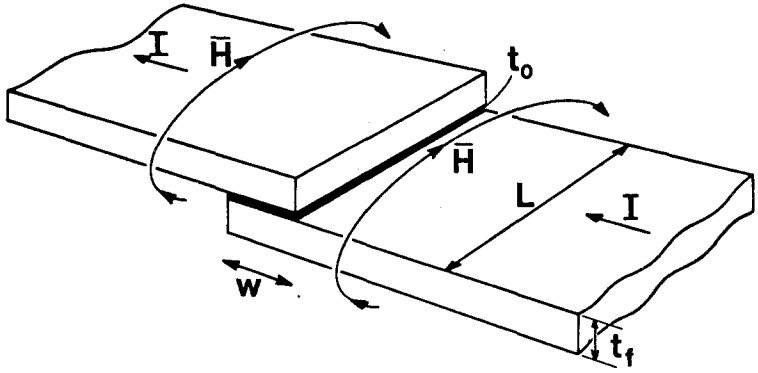

$$t_0 << \lambda_L << t_f << w << \lambda_J < L$$

$$10^{-9} \quad 5\times10^{-8} \quad 2\times10^{-7} \quad 5\times10^{-5} \quad 2\times10^{-4} \quad 10^{-3} \text{ [m]}$$

Fig. 1. Josephson tunnel junction of overlap type.

supercurrent density. The voltage across the insulating barrier is given by $V = V(x, y, t)$, the constants e and $\hbar$ are the charge of the electron and Planck's constant divided by 2π, respectively. The surface current density $\mathbf{i} = \mathbf{i}(x, y, t)$ is given by

$$\mathbf{i} = \mathbf{H} \times \mathbf{n} = \frac{1}{\mu_0} (B_x, B_y) \times \mathbf{n} = \frac{\hbar}{2ed\mu_0} \nabla\varphi \tag{2}$$

Here $d = 2\lambda_L + t_0$ is the magnetic thickness of the junction, λ_L is the London penetration depth, μ_0 is the permeability of free space, and $B_x(B_y)$ is the x component (y component) of $\mathbf{B}$. The unit vector normal to the surface is denoted $\mathbf{n}$.

The current density through the oxide layer is given by

$$j_z = j_J \sin\varphi + \frac{\hbar}{2eR} \varphi_t + \frac{\hbar C}{2e} \varphi_{tt} \tag{3}$$

The second term on the right-hand side represents dissipative effects due to quasiparticle tunneling, R being an effective normal resistance—in fact it is just Ohm's law. The third term represents the energy stored in the dielectric barrier (i.e., a displacement current).

From now on it is convenient to measure all the length x, y, t_0, λ_L, t_f, w, L, in units of the Josephson penetration depth $\lambda_J = (\hbar/2\mu_0 edj_J)^{1/2}$ and time t in units of the reciprocal plasma frequency ω_p^{-1}, where $\omega_p = (2ej_J/\hbar C)^{1/2}$. Finally, the equation of continuity

$$\nabla \cdot \mathbf{i} - j_z = 0 \tag{4}$$

substituted in (3) and using (2) yields the two-dimensional sine-Gordon equation

$$\varphi_{xx} + \varphi_{yy} = \sin\varphi + \varphi_{tt} + \alpha\varphi_t \tag{5}$$

where $\alpha = (\hbar/2eR)\,\omega_p = 1/(\beta_C)^{1/2}$, β_C is the usual McCumber parameter.

Energy input to the system is provided from the magnetic fields induced at the boundaries. In the following the boundary conditions are determined and it is shown how the two-dimensional equation is reduced to one dimension.

The magnetic field along $y = \pm w/2$ is approximately given by

$$H\left(x, \pm\frac{w}{2}, t\right) = \pm\frac{I}{2(L + t_f)\,\lambda_J j_J} \approx \pm\eta\frac{w}{2} \tag{6a}$$

or

$$\varphi_y\left(x, \pm\frac{w}{2}, t\right) = \pm\eta\frac{w}{2} = \pm\beta \tag{6b}$$

for $|x| \leqslant L/2$, where

$$\eta = \frac{I}{Lwj_J} \tag{7}$$

is the uniform bias current through the barrier. From Ampere's law it follows that

$$H\left(\pm\frac{L}{2}, y, t\right) \approx 0 \tag{8a}$$

or

$$\varphi_x\left(\pm\frac{L}{2}, y, t\right) \approx 0 \tag{8b}$$

Thus in the two-dimensional case the energy providing mechanism is the magnetic field via the boundary condition (8).

Now, a solution of the form

$$\varphi(x, y, t) = \varphi_1(x, t) + \varphi_2(y), \qquad \varphi_2 \ll 1 \tag{9}$$

reduces (5) and (6) to

$$\varphi_{1,xx} = \sin\varphi_1 + \alpha\varphi_{1,t} - \eta + \varphi_{1,tt} \tag{10}$$

which is the perturbed one-dimensional sine-Gordon equation if

$$\varphi_2(y) = \frac{\eta y^2}{2}, \qquad \frac{\eta}{2}\left(\frac{w}{2}\right)^2 \ll 1 \tag{11}$$

Thus for $\eta w^2/8 \ll 1$ the overlap geometry junction can be modeled by the damped-driven one-dimensional sine-Gordon equation. Note that η in this approximation might depend on x.

Without the perturbing damping and driving terms (10) has the famed kink/antikink solutions:

$$\varphi_{\pm}(x, t) = 4\tan^{-1}[\pm(x - x_0 - ct)/(1 - c^2)^{1/2}] \tag{12}$$

These topological solitons will exist even in the presence of damping and driving as represented by (10). The driving force will accelerate the solitons to a velocity determined by balance of the damping. This behavior can be predicted by perturbation theory[2] where the perturbation takes place around the single soliton (12). The limiting velocity is given by

$$c_\infty = \left[1 + \left(\frac{4\alpha}{\pi\eta}\right)^2\right]^{-1/2} \tag{13}$$

The soliton in a Josephson junction is thus a 2π jump in the phase difference (φ) across the insulating barrier which separates the two superconductors. Expressed in another way: It is a current loop—composed of surface current and tunneling supercurrent—connecting the two surface layers via the barrier. This current loop encompases one quantum of magnetic flux: $\Phi_0 = h/2e = 2.064 \times 10^{-15}$ V sec—and the soliton is therefore often called a fluxon.

Before moving on to the experimental manifestation of the solitons, it is worth mentioning that the Josephson junction model also can be formulated in terms of an electric equivalence diagram.[3] In this formulation the model (10) is often refered to as the resistively-shunted-junction (RSJ) model.

3. EXPERIMENTAL MANIFESTATION

Fulton and Dynes[4] suggested in 1973 that the Josephson junction could support the resonant propagation of soltions trapped in the junction. The moving soliton is accompanied by a voltage pulse [$\approx \varphi_t$ from (1b)] which can be detected at either end of the junction. The dc manifestation of the motion is a sequence of equidistantly spaced branches in the current–voltage characteristics of the junction. These near-constant voltage branches which were first reported by Chen, Finnegan, and Langenberg[5] are known as zero field steps (ZFS) because they occur in the absence of an external magnetic field. To see that the resonant motion of a soliton gives rise to a constant dc voltage, consider a single kink moving with velocity c in a junction of length L. After one full periode $T = 2L/c$ the soliton is back where it started, having been reflected at the boundaries where $\varphi_x = 0$ according to (8b). The phase φ has thus been changed by 4π in a period T. If there are N kinks in the junction the phase change will be $4N\pi$. The dc voltage is now found by integration of (1b) over one period T:

$$\frac{1}{T}\int \varphi_t \, dt = \frac{1}{T}[\varphi(T) - \varphi(0)] = \frac{2e}{\hbar} V_{dc} \tag{14}$$

from which it follows that

$$V_{dc} = \frac{4N\pi}{T}\frac{\hbar}{2e} = \frac{Nc}{L}\Phi_0 \tag{15}$$

Thus for a given value of bias current η, the dc voltage is given via (13) and (15). In fact, elimination of c from (13) and (15) gives an approximate analytic expression for the first ZFS.

The detailed dynamics of soltions in Josephson tunnel junctions have been investigated theoretically by means of analytic methodes,[6–8] perturbation analysis,[2,9,10] and numerical simulations.[11–14] An actual comparison between experimental results and numerical simulations was done in Ref. 14, while perturbation theory was compared with experiments in Ref. 10. Many of these results are reviewed in Ref. 15. The bulk of this work has shown that the perturbed sine-Gordon equation (10) is indeed a very good model describing the internal dynamics of a Josephson junction. In Fig. 2 the voltage–current characteristic of a junction of length $L=6$ is shown. The full lines are experimental results for the first three ZFS's—numerical results are indicated by circles. Excellent agreement is observed. In Fig. 3 the behavior on the first ZFS ($N=1$) is shown. A single soliton travels back and forth on the junction giving rise to a periodic voltage-pulse train of frequency $f_1 = c/2L$. On the Nth ZFS N soltions are involved and N pulses are produced within one period T. The detailed frequency spectrum of the voltage will depend on the distribution of the N pulses within the period. An example from the third ZFS is shown in Fig. 4. Figure 3 and 4 were obtained by numerical solution of a perturbed sine-Gordon equation slightly more general than (10).[14] A comparison

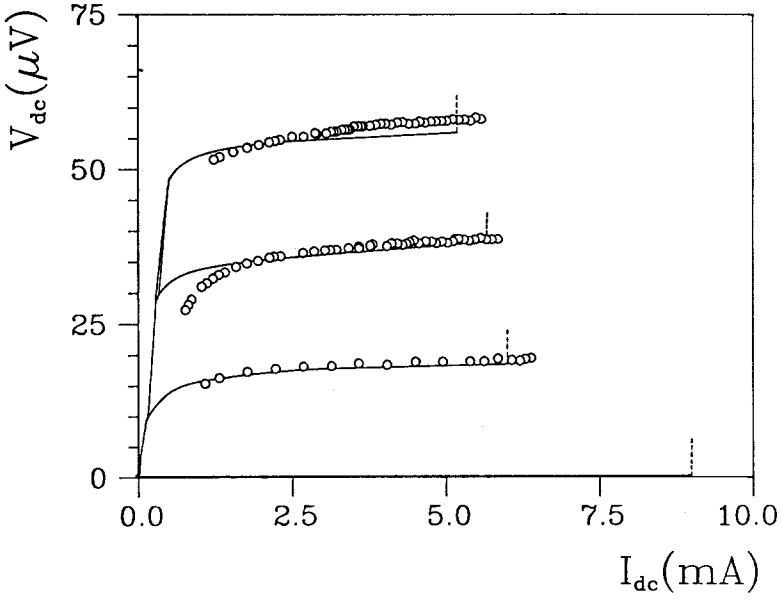

Fig. 2. The dc voltage vs. the applied bias current (η) for a Josephson junction of length $L=6$. The figure shows the first three ZFS's. Circles indicate numerical results and full lines represent the experimental results.

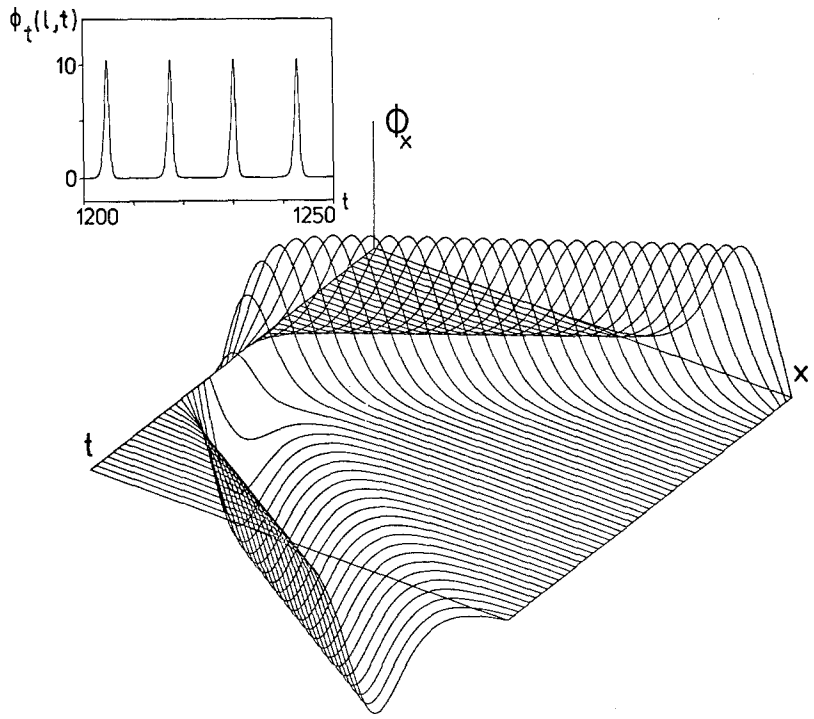

Fig. 3. Approximately one period of oscillation on the first ZFS, shown in terms of $\varphi_x(x, t)$ for ten time units. The inset shows $\varphi_t(l, t)$ for 50 time units. The length of the junction was $L \equiv 2l = 6$. The figure was obtained by numerical solution of a perturbed sine-Gordon equation[14] with $\alpha = 0.05$ and $\eta = 0.35$.

between the measured and calculated power emission at the fundamental frequency f_1 is shown in Fig. 5 versus the bias current. The calculated output power is determined through the relation $P = V^2(f_1)/2R_L$, where the load resistance R_L has been used as a fitting parameter. Using the value indicated by the arrow gives $R_L = 17k\Omega$, which indicates that the open-circuit boundary condition (8) is a good approximation. In Fig. 5 the solid curves are the numerical results and the points indicate experimental observations. The agreement is good for the first ZFS but gets worse for the second and third ZFS. However, the qualitative behavior and the relative power levels are well reproduced.

When an external magnetic field is imposed on the junction in the y direction the boundary condition (8) is no longer valid. Instead Eq. (8) will read

$$\varphi_x\left(\pm\frac{L}{2}, y, t\right) \approx \pm\beta \tag{16}$$

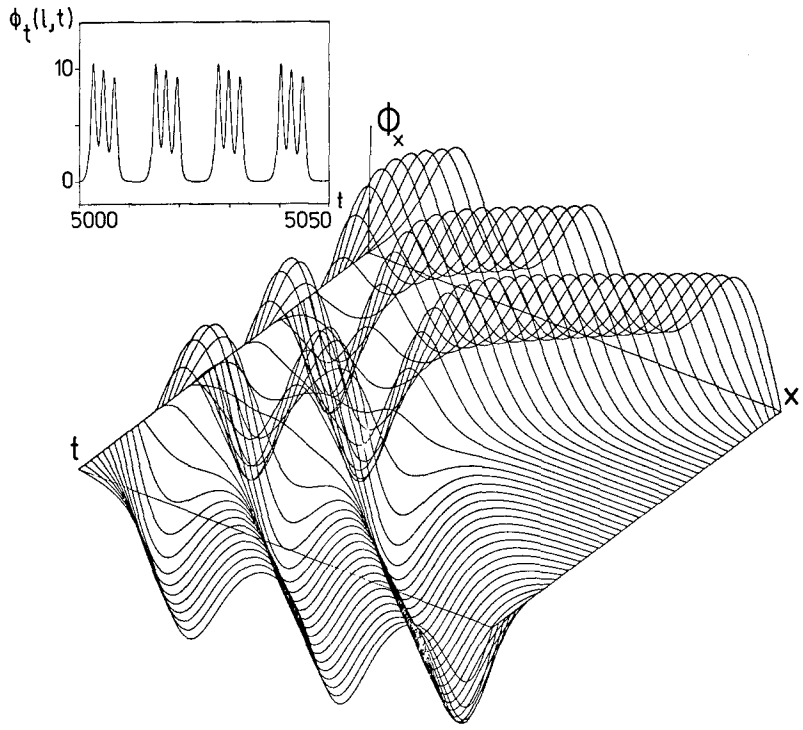

Fig. 4. Approximately one period of oscillation of the third ZFS, shown in terms of $\varphi_x(x, t)$ for ten time units. The three solitons travel 'bunched' together as one entity. The inset shows $\varphi_t(l, t)$ for 50 time units. The length of the junction was $L \equiv 2l = 6$. The figure was obtained by numerical solution of a perturbed sine-Gordon equation[14] with $\alpha = 0.05$ and $\eta = 0.35$.

where β represents the magnitude of the external magnetic field. With this type of boundary condition a simple reflection of the soliton is no longer guaranteed. For β above a certain value, numerical studies[17] show that solitons are annihilated into plasma oscillations at one end of the junction. These small-amplitude oscillations can then travel back to the other end of the junction and trigger a new soliton. The dc manifestation of this phenomena is, like for zero magnetic field, steps in the voltage–current characteristic. These steps—known as Fiske steps—thus also have an explanation in terms of soliton solutions to the perturbed sine-Gordon equation (10). Actual comparison with experimental measurements turns out to be very favorable too.[18]

The signal carried by a soliton in a Josephson junction is very weak—it is essentially given by the magnitude of the flux quantum Φ_0. This means that in order to detect a detailed wave form a rise-time-sen-

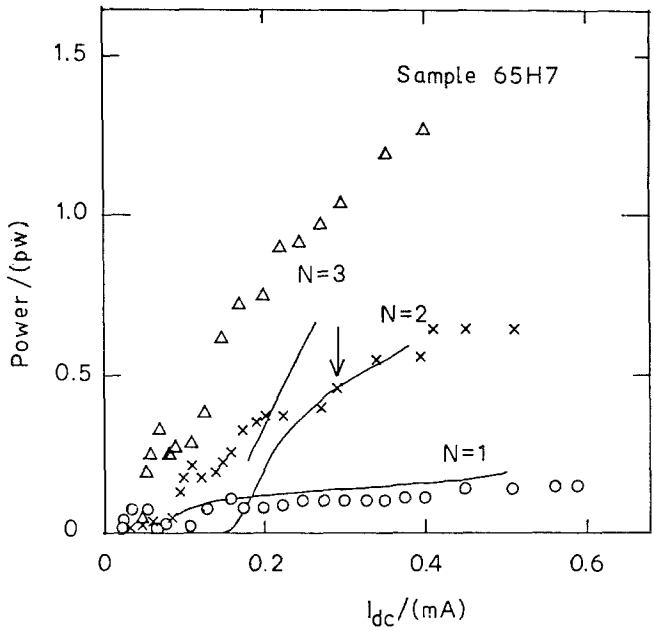

Fig. 5. Microwave power emitted from a short junction ($L=2$) at the fundamental frequency f_1. $N=1$, 2, and 3 indicates the first, second, and third ZFS, respectively. The discrete points are experimental results and the solid lines are numerical results. The arrow shows the power value used as a fitting parameter (see text).

sitivity product of less than 10^{-15} is needed for the measurement system. Recently a Japanese group reached this limit and observed for the first time the actual profile of a soliton propagating in a Josephson junction.[19,20] An input pulse with a wave form shown in Fig. 6a was applied at one end of a junction of the overlap type (Fig. 1). The output pulse detected at the other end of the junction is shown in Fig. 6b for various degrees of attenuation of the input pulse height. The number of solitons is seen to increase from one to four as the attenuation is decreased from -14 to -4 dB. These measurements have also been analyzed via the perturbed sine-Gordon equation (10), and again the agreement between experiment and model is very good.

4. CONCLUDING REMARKS

The theoretical studies of long Josephson tunnel junction dynamics mentioned in the previous section have all been done within the framework of the one-dimensional perturbed sine-Gordon equation. Detailed com-

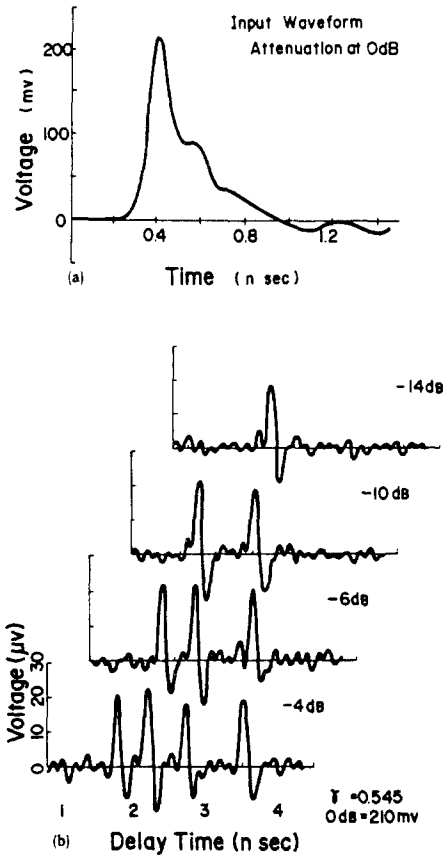

Fig. 6. Experimentally measured soliton wave form: (a) input at 0 dB; (b) output profiles as a function of input pulse height for a fixed bias current ($\eta = 0.545$). The figure is from Ref. 20.

parison with experimental results has verified that this model provides a very good description of the internal dynamics. Most experimental results indeed seem to be insensitive to the width of the junction. This is understandable when (11) is considered. Actual simulations[21,22] on the full two-dimensional model (5) have confirmed the assumptions leading to (10) and clarified the range of bias current and width values for which ZFS's are to be expected.

Because Josephson tunnel junctions have proven to be well described by one of the standard soliton equations they provide a very tractable testing ground for perturbed soliton studies. It will be interesting to see if recent theoretical studies[23] on the ac-driven sine-Gordon equation showing chaos, coherence, and interesting pattern selection rules can indeed be

observed experimentally. Josephson junctions can in this way provide feedback to our overall understanding on nonlinear phenomena, this detailed understanding of the junctions' nonlinear response should in turn make it possible to construct better design criteria for a complete integrated Josephson amplifier system, for example.[1,8]

ACKNOWLEDGMENTS

I would like to thank P. L. Christiansen, J. C. Eilbeck, O. H. Olsen, M. R. Samuelsen, and O. H. Soerensen for contributions to this work. The work was done under the auspices of the U.S. Department of energy.

REFERENCES

1. A. Barone and G. Paterno, *Physics and Applications of the Josephson Effect* (John Wiley, New York, 1982).
2. D. W. McLaughlin and A. C. Scott, *Phys. Rev. A* **18**:1652 (1978).
3. A. C. Scott, F. Y. F. Chu, and S. A. Reible, *J. Appl. Phys.* **47**:3272 (1976).
4. T. A. Fulton and R. C. Dynes, *Solid State Commun.* **12**:57 (1973).
5. J. T. Chen, T. F. Finnegan, and D. N. Langenberg, *Physica* **55**:413 (1971).
6. G. Costabile, R. D. Parmentier, B. Savo, D. W. McLaughlin, and A. C. Scott, *Appl. Phys. Lett.* **32**:587 (1978).
7. R. M. DeLeonardis, S. E. Trullinger, and R. F. Wallis, *J. Appl. Phys.* **51**:587 (1978).
8. R. D. Parmentier, in *Solitons in Action*, K. Lonngren and A. C. Scott, eds. (Academic Press, New York, 1978), p. 173.
9. O. A. Levring, N. F. Pedersen, and M. R. Samuelsen, *J. Appl. Phys.* **54**:987 (1983).
10. N. F. Pedersen and D. Welner, *Phys. Rev. B* **29**:2551 (1984).
11. K. Nakajima, T. Yamashita, and Y. Onodera, *J. Appl. Phys.* **45**:3141 (1974).
12. K. Nakajima, Y. Onodera, T. Nakamura, and R. Sato, *J. Appl. Phys.* **45**:4095 (1974).
13. S. N. Erne and R. D. Parmentier, *J. Appl. Phys.* **51**:5025 (1980); **52**:1608 (1981).
14. P. S. Lomdahl, O. H. Soerensen, and P. L. Christiansen, *Phys. Rev. B* **25**:5737 (1982).
15. N. F. Pedersen, Solitons in Long Josephson Junctions, in *NATO Advanced Study Institute Series, Proceedings of the 1982 Summer School, Erice, Italy* (Plenum Press, New York, 1983).
16. B. Dueholm *et al.*, *Phys. Rev. Lett.* **46**:1299 (1981).
17. O. A. Levring *et al.*, *Physica Scripta* **25**:810 (1982).
18. M. P. Sorensen *et al.*, *Phys. Rev. B* **30**:2640 (1985).
19. A. Matsuda and T. Kawakami, *Phys. Rev. Lett.* **51**:694 (1983).
20. J. Nitta, A. Matsuda, and T. Kawakami, *J. Appl. Phys.* **55**:2758 (1984).
21. J. C. Eilbeck, P. S. Lomdahl, O. H. Olsen, and M. R. Samuelsen, *J. Appl. Phys.* **57**:861 (1985).
22. P. S. Lomdahl, O. H. Olsen, J. C. Eilbeck, and M. R. Samuelsen, *J. Appl. Phys.* **57**:997 (1985).
23. A. R. Bishop, K. Fesser, P. S. Lomdahl, W. C. Kerr, M. B. Williams, and S. E. Trullinger, *Phys. Rev. Lett.* **50**:1095 (1983).